- Hydrolytic Activities of Crystalline Cellulose Nanofibers
  Serizawa, T.; Sawada, T.; Okura, H.; Wada, M. *Biomacromolecules* **2013**, *14*, 613-617.
  Abstract:

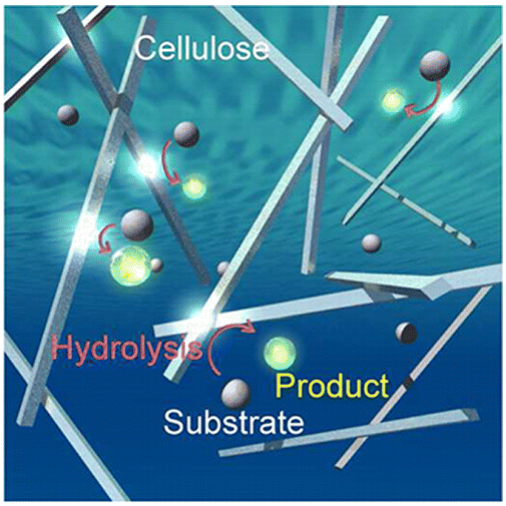

Cellulose is commonly believed to be inactive to organic substances; this inertness is an essential requirement for raw materials in industrial products. Here we demonstrate the contradictory but promising properties, which are the hydrolytic activities of crystalline cellulose nanofibers for the ester, monophosphate, and even amide bonds of small organic substrates under extremely mild conditions (neutral pH, moderate temperature, and atmospheric pressure). The hydrolytic activities were significantly extended to decompose the coat proteins of model viruses, followed by a drastic decrease in their infection capabilities to the host cells.

- Self-assembled amphiphilic DNA-cholesterol/DNA-peptide hybrid duplexes with liposome-like structure for doxorubicin delivery
  Choi, K.-M.; Kwon, I. C.; Ahn, H. J. *Biomaterials* **2013**, *34*, 4183-4190.
  Abstract:

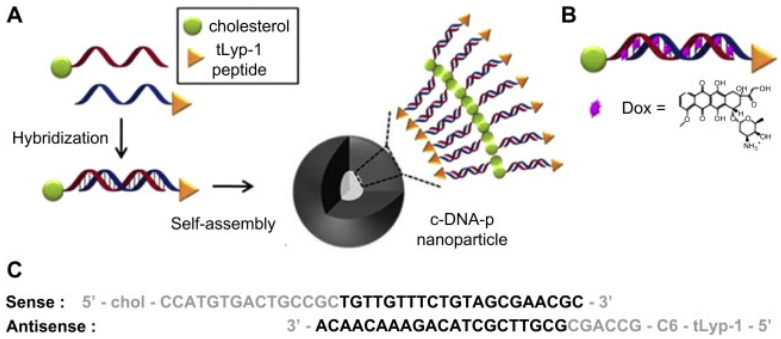

DNA nanoparticles have been proposed for drug encapsulation and intracellular delivery, but it has remained a challenge to rationally design DNA nanoparticles for delivery of drug to human cancer cells, not to normal cells. In this study, we synthesized an amphiphilic DNA hybrid duplex by using Watson–Crick base pairing and DNA bioconjugation with cholesterol or tLyp-1 tumor-homing peptide. The resulting amphiphilic DNA hybrid duplexes can self-assemble in an aqueous solution into liposome-like nanoparticles (c-DNA-p nanoparticles) with the exposure of tLyp-1 peptides to their outside. As a nanocarrier for doxorubicin, c-DNA-p nanoparticles can efficiently intercalate doxorubicin and also show the pH-dependent complexing/dissociation behaviors with doxorubicin, resulting in release of doxorubicin into cytosol after cell uptake. Moreover, tLyp-1 peptides with cell penetrating properties and specific binding ability for Neuropilin-1 receptors enable doxorubicin-

loaded c-DNA-p nanoparticles to be delivered into the target cells through the NRP-1-dependent internalization pathway. Here, we demonstrated the targeted delivery of doxorubicin to MDA-MB231 breast cancer cells, compared to HFF normal cells. These results provide an alternative approach to specifically delivering doxorubicin into targeted cells for cancer therapy as well as controlling drug release under the acidic conditions such as endosomes or lysosomes.

- Between Superexchange and Hopping: An Intermediate Charge-Transfer Mechanism in Poly(A)-Poly(T) DNA Hairpins
  Renaud, N.; Berlin, I.A.; Lewis, F. D.; Ratner, M. A. *J. Am. Chem. Soc.* **2013**, *135*, 3953–3963.
  Abstract:

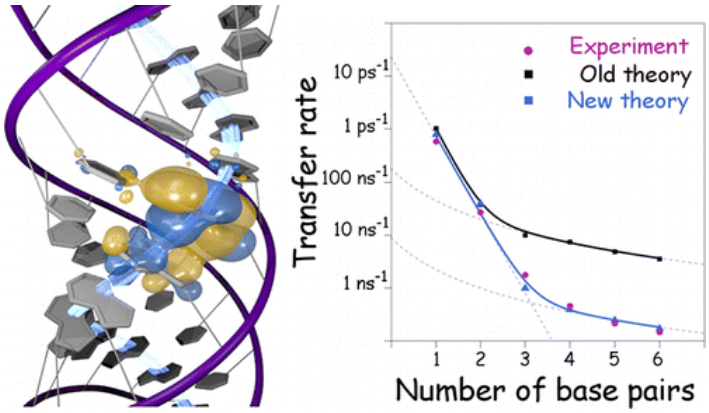

We developed a model for hole migration along relatively short DNA hairpins with fewer that seven adenine (A):thymine (T) base pairs. The model was used to simulate hole migration along poly(A)-poly(T) sequences with a particular emphasis on the impact of partial hole localization on the different rate processes. The simulations, performed within the framework of the stochastic surrogate Hamiltonian approach, give values for the arrival rate in good agreement with experimental data. Theoretical results obtained for hairpins with fewer than three A:T base pairs suggest that hole transfer along short hairpins occurs via superexchange. This mechanism is characterized by the exponential distance dependence of the arrival rate on the donor/acceptor distance, ka e–βR, with β = 0.9 Å–1. For longer systems, up to six A:T pairs, the distance dependence follows a power law ka R–η with η = 2. Despite this seemingly clear signature of unbiased hopping, our simulations show the complete delocalization of the hole density along the entire hairpin. According to our analysis, the hole transfer along relatively long sequences may proceed through a mechanism which is distinct from both coherent single-step superexchange and incoherent multistep hopping. The criterion for the validity of this mechanism intermediate between superexchange and hopping is proposed. The impact of partial localization on the rate of hole transfer between neighboring A bases was also investigated.

- Transformation from Kinetically into Thermodynamically Controlled Self-Organization of Complex Helical Columns with 3D Periodicity Assembled from Dendronized Perylene Bisimides
  Percec, V.; Sun, H.-J.; Leowanawat, P.; Peterca, M.; Graf, R.; Spiess, H. W.; Zeng, X.; Ungar, G.; Heiney, P. A. *J. Am. Chem. Soc.* **2013**, *135,* 4129–4148.
  Abstract:

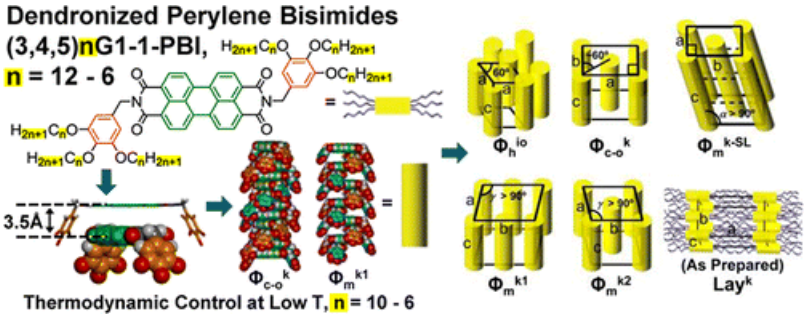

The dendronized perylene 3,4:9,10-tetracarboxylic acid bisimide (PBI), (3,4,5)12G1-1-PBI, was reported by our laboratory to self-assemble into complex helical columns containing dimers of dendronized PBI with one molecule in each stratum, with different intra- and interdimer rotation angles but identical intra- and interdimer distance of 3.5 Å, exhibiting a four-strata 21 helical repeat. A thermodynamically controlled 2D columnar hexagonal phase with short-range intracolumnar order represents the thermodynamic product at high temperature, while a kinetically controlled monoclinic columnar array with 3D periodicity is the thermodynamic product at low temperature. With heating and cooling rates higher than 10 °C/min to 1 °C/min, at low temperature the 2D columnar periodic array is the kinetic product for this dendronized PBI. Here the synthesis and structural analysis of a library of (3,4,5)nG1-m-PBI with n = 12 to 6 and m = 1 are reported. A combination of differential scanning calorimetry, X-ray diffraction on powder and orientated fibers, including pattern simulation and electron density map reconstruction, and solid-state NMR, all as a function of temperature and heating and cooling rate, was employed for their structural analysis. It was discovered that at low temperature the as-prepared n = 12 to 10 exhibit a 3D layered array that transforms irreversibly into columnar periodicities during heating and cooling. Also the kinetically controlled 3D columnar phase of n = 12 becomes thermodynamically controlled for n = 10, 9, 8, 7, and 6. This unprecedented transformation is expected to facilitate the design of functions from dendronized PBI and other self-assembling building blocks.

- Extending the Limits of Precision Polymer Synthesis: Giant Polyphenylene Dendrimers in the Megadalton Mass Range Approaching Structural Perfection
  Nguyen, T.-T.-T.; Baumgarten, M.; Rouhanipour, A.; Räder, H. J.; Lieberwirth, I.; Müllen; K. *J. Am. Chem. Soc.* **2013**, *135*, 4183–4186.
  Abstract:

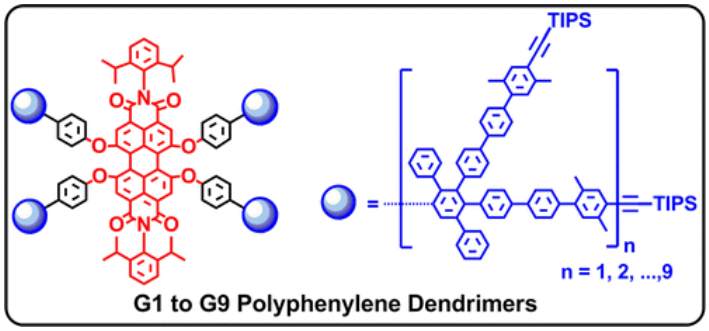

The catalyst-free Diels–Alder synthesis of polyphenylene dendrimers with a chromophore core has now been demonstrated to achieve the seventh to ninth generations upon divergent growth. Since standard analytical tools such as size-exclusion chromatography do not provide realistic molecular weights, MALDI-TOF mass spectrometry was applied to characterize the complete series of nine generations. Perfection and monodispersity were thus elucidated at such high masses. Transmission

electron microscopy imaging was used to determine the size of these molecularly defined nanosized "particles" with diameters of up to 33 nm.

- Synthesis and Properties of Two Cationic Narrow Band Gap Conjugated Polyelectrolytes
  Henson, Z. B.; Zhang, Y.; Nguyen, T.-Q.; Seo, J. H.; Bazan, G. C. *J. Am. Chem. Soc.* **2013**, *135*, 4163–4166.
  Abstract:

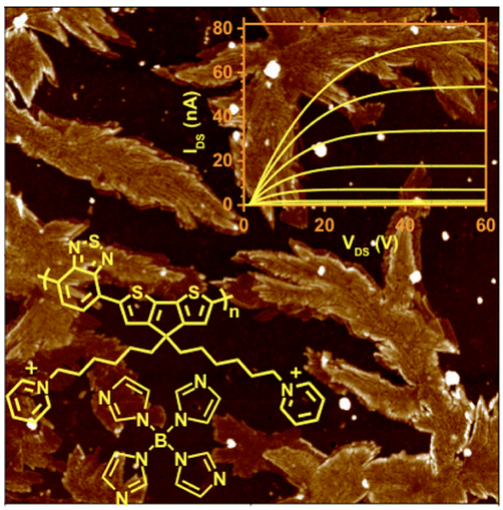

We report the design, synthesis, and optical and electronic properties of two novel narrow band gap conjugated polyelectrolytes (NBGCPEs) based on a poly[2,6-(4,4-bis-alkyl-4*H*-cyclopenta[2,1-*b*;3,4-*b*]dithiophene)-*alt*-4,7-(2,1,3-benzothiadiazole)] donor/acceptor backbone. Comparison with the properties of the neutral precursor material shows that the ionic component in these cationic NBGCPEs leads to a red-shift in the absorption spectra and to a modification of the polymer electronic energy levels. Both the HOMO and the LUMO are lowered in energy, with the net effect being dependent on the choice of counterion, i.e. bromide vs tetrakis(1-imidazolyl)borate. Moreover, we unexpectedly find n-type transport in thin-film transistors, as opposed to the widely studied p-type transport in neutral systems with isoelectronic backbones. From these observations we conclude that introduction of ionic functionalities adjacent to semiconducting polymers that exhibit charge-transfer excitations offers unique opportunities for materials design.

- Molecular Imaging by Optically Detected Electron Spin Resonance of Nitrogen-Vacancies in Nanodiamonds
  Hegyi, A.; Yablonovitch, E. *Nano Lett.* **2013**, *13*, 1173-1178.
  Abstract:

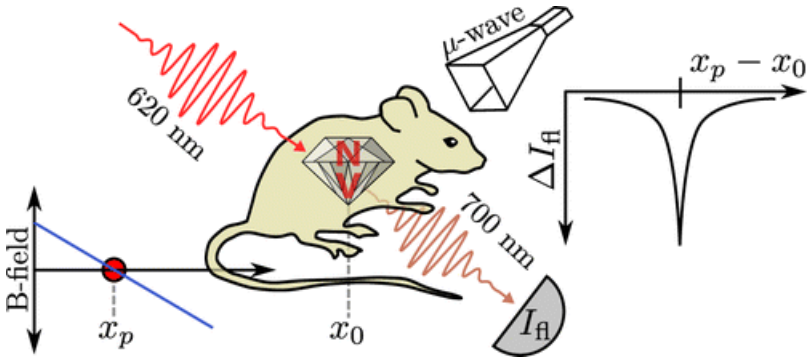

We propose a novel biomedical imaging technique, called nanodiamond imaging, that noninvasively

records the three-dimensional distribution of biologically tagged nanodiamonds in vivo. Our technique performs optically detected electron spin resonance of nitrogen-vacancy centers in nanodiamonds, a nontoxic nanomaterial that is easily biologically functionalized. We demonstrate the feasibility of the technique by imaging multiple nanodiamond targets within pieces of chicken breast; it is the first demonstration of imaging within scattering tissue by optically detected magnetic resonance. We achieve a sensitivity equivalent to 740 pg of nanodiamond in 100 s of measurement time and a spatial resolution of 800 µm over a 1 cm^2 field of view, and we show how the technique has the potential to yield images with combined high sensitivity (100 fg nanodiamond) AND high spatial resolution (100 µm) over organism-scale fields of view, features which are mutually exclusive in existing imaging modalities except at the shallowest imaging depths.

- Frequency-Multiplication High-Output Triboelectric Nanogenerator for Sustainably Powering Biomedical Microsystems
  Zhang, X.-S.; Han, M.-D.; Wang, R.-X.; Zhu, F.-Y.; Li, Z.-H.; Wang, W.; Zhang, H.-X. *Nano Lett.* **2013**, *13*, 1168-1172.
  Abstract:

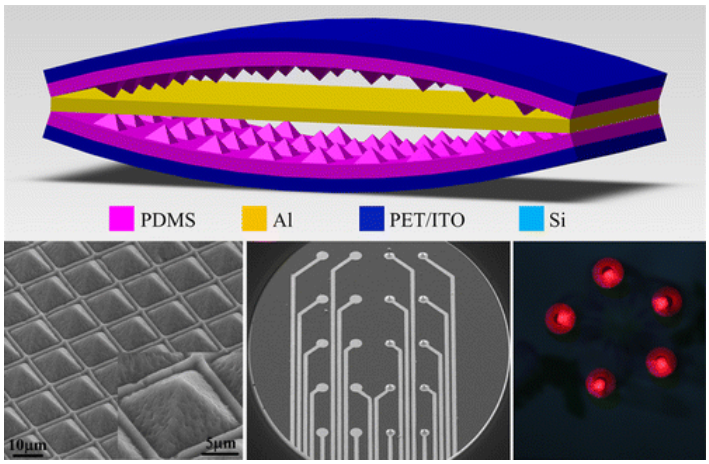

An attractive method to response the current energy crisis and produce sustainable nonpolluting power source is harvesting energy from our living environment. However, the energy in our living environment always exists in low-frequency form, which is very difficult to be utilized directly. Here, we demonstrated a novel sandwich-shape triboelectric nanogenerator to convert low-frequency mechanical energy to electric energy with double frequency. An aluminum film was placed between two polydimethylsiloxane (PDMS) membranes to realize frequency multiplication by twice contact electrifications within one cycle of external force. The working mechanism was studied by finite element simulation. Additionally, the well-designed micro/nano dual-scale structures (i.e., pyramids and V-shape grooves) fabricated atop PDMS surface was employed to enhance the device performance. The output peak voltage, current density, and energy volume density achieved 465 V, 13.4 µA/cm2, and 53.4 mW/cm3, respectively. This novel nanogenerator was systematically investigated and also demonstrated as a reliable power source, which can be directly used to not only lighten five commercial light-emitting diodes (LEDs) but also drive an implantable 3-D microelectrode array for neural prosthesis without any energy storage unit or rectification circuit. This is the first demonstration of the nanogenerator for directly driving biomedical microsystems, which extends the application fields of the nanogenerator and drives it closer to practical applications.

- Helical Colloidal Sphere Structures through Thermo-Reversible Co-Assembly with Molecular Microtubes
  Jiang, L.; de Folter, J. W. J.; Huang, J.; Philipse, A. P.; Kegel, W. K.; Petukhov, A. V. *Angew. Chem. Int. Ed.* **2013**, *52*, 3364 –3368.
  Abstract:

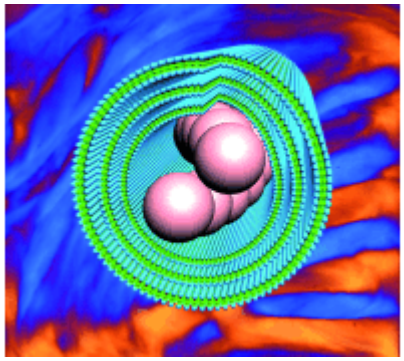

The co-assembly of spherical colloids and surfactant–cyclodextrin microtubes yields a library of dynamic colloid-in-tube structures, including helices. In situ observations of these structures, including their thermo-reversible assembly and disassembly, demonstrate the potential of the interplay between molecular and colloidal self-assembly, thereby providing a novel route to temperature-sensitive particle alignment and release.

- Multivalent Directed Assembly of Colloidal Particles
  Ejima, H.; Richardson, J. J.; Caruso, F. *Angew. Chem. Int. Ed.* **2013**, *12*, 3314-3316.
  Abstract:

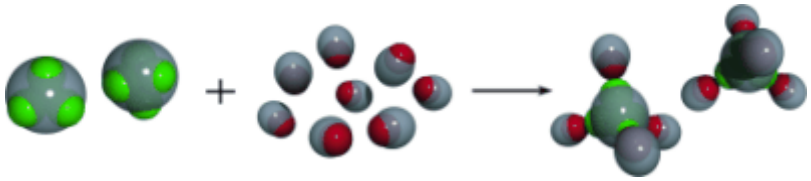

Sticking together: Colloidal particles with a determined number of sticky sites arranged in precise geometries analogous to atoms were created. The kinetics of the colloidal assemblies related to specific chemical reactions (see figure) were investigated using optical microscopy. This general method should allow for a broad range of useful 3D colloidal assemblies.

- Phosphacycles as Building Blocks for Main Group Cages
  Townsend, N. S.; Shadbolt, S. R.; Green, M.; Russel, C. A. *Angew. Chem. Int. Ed.* **2013**, *12*, 3481-3484.
  Abstract:

Cationic pnictogen/carbon cages are formed from reaction of 2,4,6-tri-*tert*-butyl-1,3,5-triphosphabenzene with the carbene mimics EX_2^+ (E=P, As). For E=P, 1,4-addition to the hetereoaromatic compound is observed, whereas for E=As, cage complexes are formed.

- A Small-Molecule Zwitterionic Electrolyte without a π-Delocalized Unit as a Charge-Injection Layer for High-Performance PLEDs
  Min, C.; Shi, C.; Zhang, W.; Jiu, T.; Chen, J.; Ma, D.; Fang, J. *Angew. Chem. Int. Ed.* **2013**, *52*, 3417 –3420.
  Abstract:

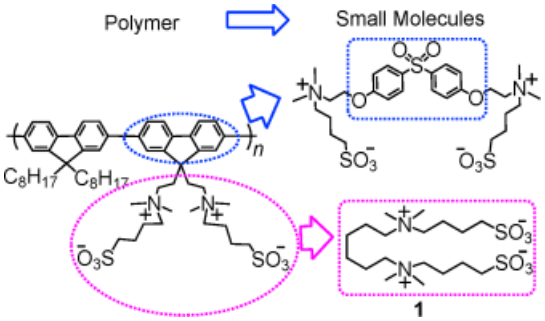

1

Down to the bare bones: Small-molecule zwitterionic materials were found to be more efficient as charge-injection materials in an organic electronic device than a previously described polymer (see structures). Furthermore, the superior device performance observed for 1 indicates that it is not necessary to focus only on π-delocalized systems and that solid ionic liquids may be promising alternative candidates for charge-injection materials.

- Evidence for Kinetic Nucleation in Helical Nanofiber Formation Directed by Chiral Solvent for a Perylene Bisimide Organogelator
  Stepanenko, V.; Li, X.-Q.; Gershberg, J.; Würthner, F. *Chem. Eur. J.* **2013**, *19*, 4176–4183.
  Abstract:

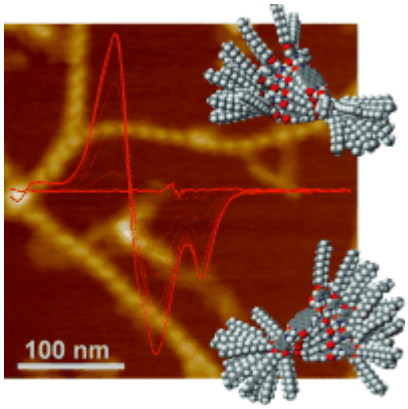

The self-assembly behavior of an achiral perylene bisimide (PBI) organogelator that bears two 3,4,5-tridodecyloxybenzoylaminoethyl substituents at the imide positions has been investigated in chiral solvents (*R*)- and (*S*)-limonene in great detail by circular dichroism (CD) spectroscopy and atomic force microscopy (AFM). CD spectroscopic studies on dilute solutions revealed a preferential population of one-handed helical assemblies in chiral solvent with an enantiomeric excess close to 100 %, whereas AFM images of more than 100 nanofibers of the organogel obtained from more concentrated solutions were found to consist of both handed helices with an enantiomeric excess of only 20 %. This discrepancy is attributed to the fast gelation process at high dye concentration that evidently proceeds through non-equilibrated nuclei in a kinetic rather than thermodynamic self-assembly process. Under these conditions the chiral induction from the homochiral solvent may not be adequate in effectively populating only one-handed helices.

- Kinetic Resolution of Planar-Chiral 1,2-Disubstituted Ferrocenes by Molybdenum-Catalyzed Asymmetric Intraannular Ring-Closing Metathesis
  Ogasawara, M.; Arae, S.; Watanabe, S.; Nakajima, K.; Takahashi, T. *Chem. Eur. J.* **2013**, *19*, 4151–4154.
  Abstract:

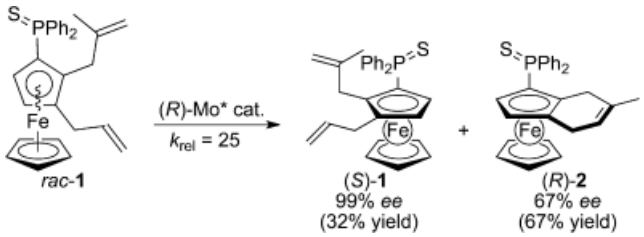

Planar chirality: Ring-closing metathesis of 1,2-diallylmetallocenes afforded the corresponding 4,7-dihydroindenyl species in high yields. The metallocenes are planar chiral with two different allylic substituents, and kinetic resolution of the racemic 1,2-diallylmetallocene derivatives was realized by molybdenum-catalyzed asymmetric ring-closing metathesis with excellent enantioselectivity (see scheme).

- Salt-specific effects in aqueous dispersions of carbon nanotubes
  Suttipong, M.; Tummala, N. R.; Striolo, A.; Batista, C. S.; Fagan, J. *Soft Matter* **2013**, *9*, 3712-3719.
  Abstract:

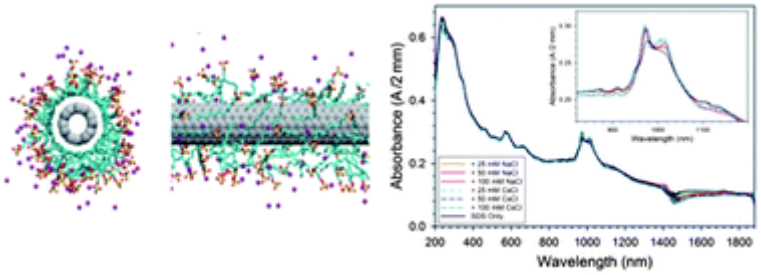

Tremendous progress has been made to stabilize carbon nanotube dispersions using surfactants, although many questions await answer to design surfactant formulations that selectively stabilize nanotubes mono-dispersed in diameter and chirality. Stimulated by recent experimental observations [*J. Am. Chem. Soc.*, 2010, **132**, 16165–16175], we attempt here to quantify how changing the counter-ion (Cs^+ instead of Na^+) affects the morphology of dodecyl sulfate surfactants adsorbed on carbon nanotubes. Using atomistic molecular dynamics we simulated aqueous cesium dodecyl sulfate (CsDS) adsorbed on (6,6), (12,12), and (20,20) single-walled carbon nanotubes (SWCNTs) at ambient conditions. When compared to results for sodium dodecyl sulfate (SDS), our results suggest that surface aggregates with Cs^+ ions, compared to Na^+, yield a more compact coverage of the nanotubes at the surfactant surface coverage of 0.25 nm^2 per headgroup, with the surfactant heads extended towards the bulk aqueous solution, and prevent water from accessing the nanotube surface. These morphological results suggest that CsDS should be more effective than SDS at stabilizing aqueous carbon nanotubes dispersions. More importantly, these results were obtained only for the (6,6) nanotubes simulated. For the wider nanotubes our simulations show limited, if any, differences in the morphology of the surfactant aggregates when the Na^+ ions are substituted with Cs^+ ones. To validate our results we measured experimental UV-Vis-NIR absorbance spectra for aqueous carbon nanotubes with diameters similar to that of (6,6) and of (12,12) nanotubes stabilized by SDS at increasing salt concentration (CsCl *vs.* NaCl). The results are indicative of changes in the

surfactant self-assembled structure on the narrow nanotubes in the presence of Cs^+ ions, while data for the wider tubes only suggest salt-screening effects for both Na^+ and Cs^+ ions. The different salt-specific behavior observed for the surfactants adsorbed on narrow *vs.* wide carbon nanotubes could be exploited for the selective stabilization of mono-dispersed carbon nanotube samples, although a surfactant more effective than SDS should be used.

- Emergent colloidal dynamics in electromagnetic fields
  Dobnikar, J.; Snezhko, A.; Yethiraj, A. *Soft Matter* **2013**, *9*, 3693-3704.
  Abstract:

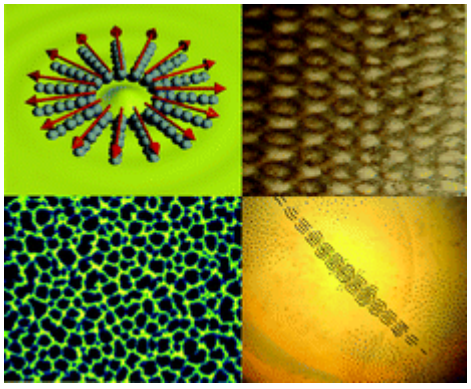

We present a current review of the collective dynamics that can arise in colloidal systems subjected to electromagnetic fields. The focus is on phenomena that are not simply understandable purely from a dipolar model, but instead emerge from the collective behavior of many discrete interacting components driven out of equilibrium by external forces. We examine in particular the fascinating diversity of large-scale dynamical structures that arise due to the interplay between the induced interactions, time-dependent energy injection, and coupling with the fluid flow.

- Designed 3D architectures of high-temperature superconductors
  Green, D. C.; Lees, M. R.; Hall, S. R. *Chem. Commun*. **2013**, *49*, 2753-2755.
  Abstract:

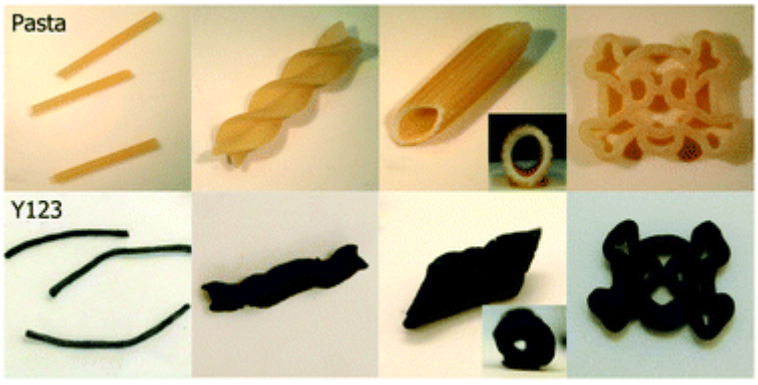

Self-supporting superconducting replicas of pasta shapes are reported, yielding products of differing 3D architectures. Functioning high-temperature superconductor wires are developed and refined from replicas of spaghetti, demonstrating a unique sol–gel processing technique for the design and synthesis of novel macroscopic morphologies of complex functional materials.

- Meniscus confined fabrication of multidimensional conducting polymer nanostructures with scanning electrochemical cell microscopy (SECCM)

McKelvey, K.; O'Connell, M. A.; Unwin, P. R. *Chem. Commun*. **2013**, *49*, 2986-2988.
Abstract:

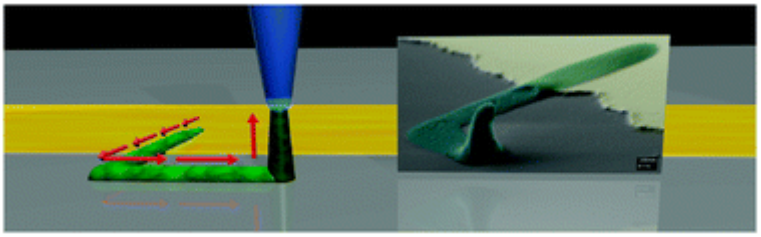

Scanning electrochemical cell microscopy (SECCM) is demonstrated as a new approach for the construction of extended multi-dimensional conducting polymer (polyaniline) nanostructures, making use of a mobile dual-channel theta pipette cell to control and monitor the location, rate and extent of electropolymerisation.

- Three-dimensional optical manipulation of a single electron spin
  Geiselmann, M.; Juan, M. L.; Renger, J.; Say, J. M.; Brown, L. J.; De Abajo, F. J. G.; Koppens, F.; Quidant, R. *Nature Nano.* **2013**, *8*, 175–179.
  Abstract:

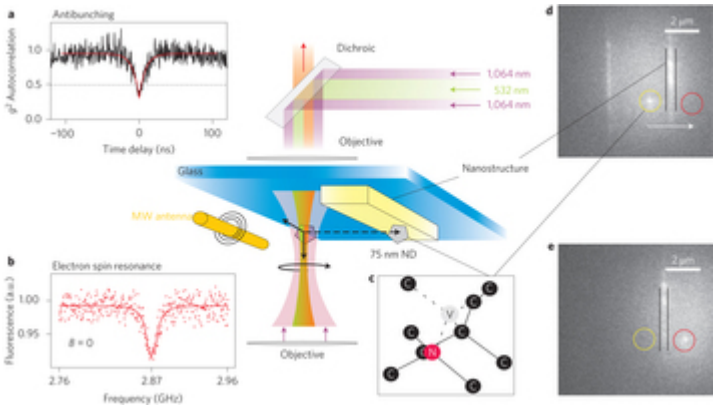

Nitrogen vacancy (NV) centres in diamond are promising elemental blocks for quantum optics, spin-based quantum information processing and high-resolution sensing. However, fully exploiting the capabilities of these NV centres requires suitable strategies to accurately manipulate them. Here, we use optical tweezers as a tool to achieve deterministic trapping and three-dimensional spatial manipulation of individual nanodiamonds hosting a single NV spin. Remarkably, we find that the NV axis is nearly fixed inside the trap and can be controlled *in situ* by adjusting the polarization of the trapping light. By combining this unique spatial and angular control with coherent manipulation of the NV spin and fluorescence lifetime measurements near an integrated photonic system, we demonstrate individual optically trapped NV centres as a novel route for both three-dimensional vectorial magnetometry and sensing of the local density of optical states.

- Dynamic control of magnetic nanowires by light-induced domain-wall kickoffs
  Heintze, E.; El Hallak, F.; Clauß, C.; Rettori, A.; Pini, M. G.; Totti, F.; Dressel, M.; Bogani, L. *Nature Mater.* **2013**, *12*, 202–206.
  Abstract:

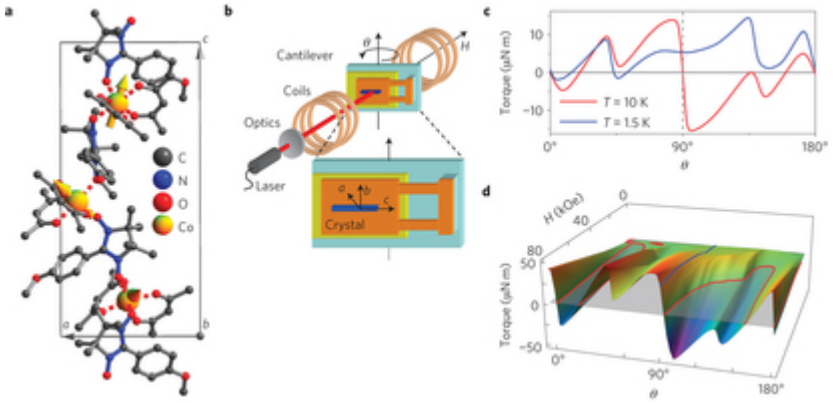

Controlling the speed at which systems evolve is a challenge shared by all disciplines, and otherwise unrelated areas use common theoretical frameworks towards this goal. A particularly widespread model is Glauber dynamics, which describes the time evolution of the Ising model and can be applied to any binary system. Here we show, using molecular nanowires under irradiation, that Glauber dynamics can be controlled by a novel domain-wall kickoff mechanism. In contrast to known processes, the kickoff has unambiguous fingerprints, slowing down the spin-flip attempt rate by several orders of magnitude, and following a scaling law. The required irradiance is very low, a substantial improvement over present methods of magneto-optical switching. These results provide a new way to control and study stochastic dynamic processes. Being general for Glauber dynamics, they can be extended to different kinds of magnetic nanowires and to numerous fields, ranging from social evolution[2] to neural networks and chemical reactivity.

- Blue-Emitting Butterfly-Shaped 1,3,5,9-Tetraarylpyrenes: Synthesis, Crystal Structures, and Photophysical Properties
  Feng, X.; Hu, J.-Y.; Iwanaga, F.; Seto, N.; Redshaw, C.; Elsegood, M. R. J.; Yamato, T. *Org. Lett.* **2013**, *15*, 1318-1321.
  Abstract:

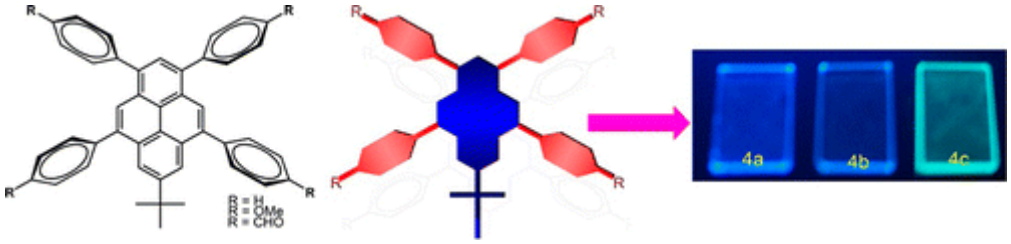

The first example of aryl-functionalized, butterfly-shaped, highly fluorescent and stable blue-emitting monomers, namely, 7-tert-butyl-1,3,5,9-tetrakis(p-R-phenyl)pyrenes, were synthesized by the SuzukiMiyaura cross-coupling reaction from a novel bromide precursor of 1,3,5,9-tetrabromo-7-tert-butylpyrene. The crystal structures and optical and electronic properties have been investigated.

- Cyanated Diazatetracene Diimides with Ultrahigh Electron Affinity for n‑Channel Field Effect Transistors
  Ye, Q.; Chang, J.; Huang, K.-W.; Shi, X.; Wu, J.; Chi, C. *Org. Lett.* **2013**, *15*, 1194-1187.
  Abstract:

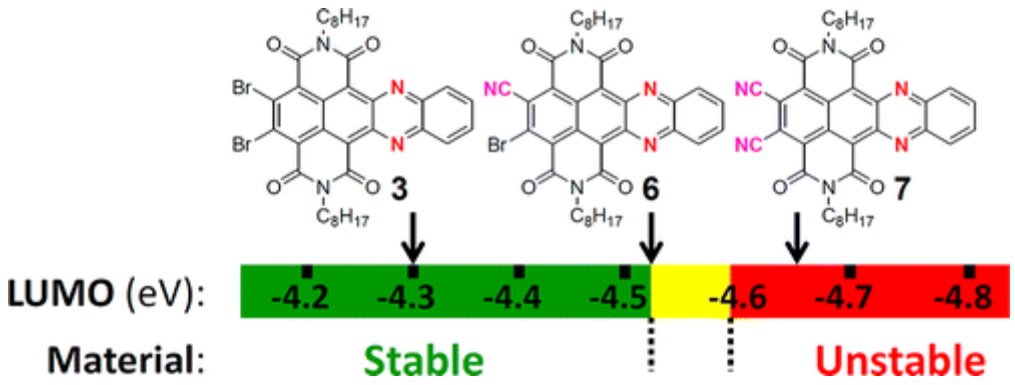

Several diazatetracene diimides with high electron affinity (up to 4.66 eV!) were prepared and well characterized. The LUMO energy level of these electron-deficient molecules was found to be closely related to their material stability. Compound 7 with ultrahigh electron affinity suffered from reduction and hydrolysis in the presence of silica gel or water. The stable compounds 3 and 6 showed n-channel FET behavior with an average electron mobility of 0.002 and 0.005 $cm^2V^{-1}s^{-1}$, respectively, using a solution processing method.

- Converting an Electrical Insulator into a Dielectric Capacitor: End-Capping Polystyrene with Oligoaniline
  Hardy, C. G.; Islam, M. S.; Gonzalez-Delozier, D.; Morgan, J. E.; Cash, B.; Benicewicz, B. C.; Ploehn, H. J.; Tang, C. *Chem. Mater.* **2013**, *25*, 799-807.
  Abstract:

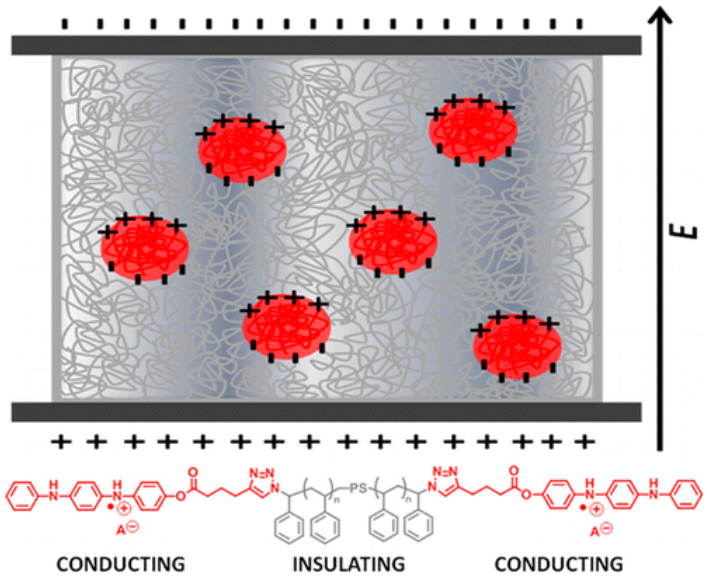

We report a simple and low-cost strategy to enhance the dielectric permittivity of polystyrene by up to an order of magnitude via incorporating an oligoaniline trimer moiety at the end of the polymer chains. The oligoaniline-capped polystyrene was prepared by a copper-catalyzed click reaction between azide-capped polystyrene and an alkyne-containing aniline trimer, which was doped by different acids. By controlling molecular weight of polystyrene, the end-capped polymers can be induced to form nanoscale oligoaniline-rich domains embedded in an insulating matrix. Under an external electric field, this led to an increase in dielectric polarizability while maintaining a low dielectric loss. At frequencies as high as 0.1 MHz, the dielectric permittivity and dielectric loss (tan δ) were ~22.8 and ~0.02, respectively. This strategy may open a new avenue to increasing the dielectric permittivity of many other commodity polymers while maintaining relatively low dielectric

loss.

- Self-Assembled Monolayers Based Upon a Zirconium Phosphate Platform
  Díaz, A.; Mosby, B. M.; Bakhmutov, V. I.; Martí, A. A.; Batteas, J. D.; Clearfield, A. *Chem. Mater.* **2013**, *25*, 723-728.
  Abstract:

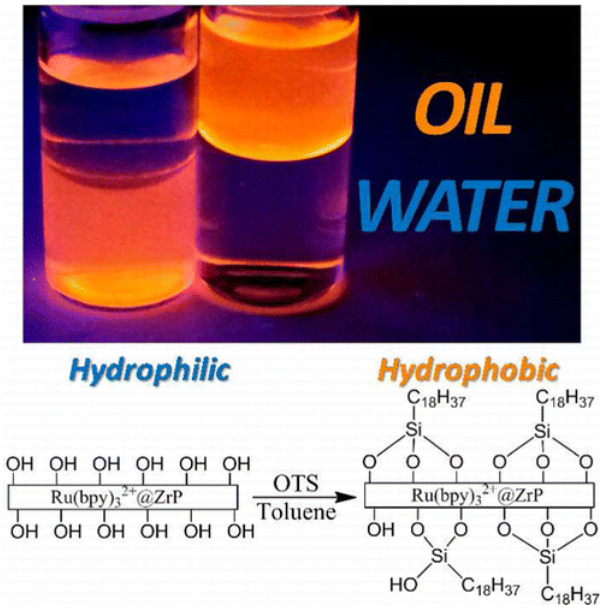

Organically surface-modified α-zirconium phosphate was obtained by reacting the surface P–O–H groups of α-zirconium phosphate nanoparticles (α-ZrP) with octadecyltrichlorosilane (OTS). Surface functionalization of α-ZrP with OTS was accomplished using a one-step synthesis producing highly hydrophobic nanoparticles. The formation of P–O–Si bonds arising from nucleophilic attack of POH to the silane was confirmed by solid-state NMR experiments. The surface coverage of the organic modifier was characterized by TGA, AFM, and FTIR. In addition, we show the applicability of this system with a photoinduced electron-transfer reaction in a nonpolar solvent. Using an organically surface-modified α-ZrP previously loaded with tris(2,2′-bipyridyl)ruthenium(II) ($Ru(bpy)_3^{2+}$), the quenching of the luminescence of $Ru(bpy)_3^{2+}$ in the presence of p-benzoquinone was monitored; a static quenching constant (K_s) value of 8.82×10^2 M^{-1} and a dynamic quenching constant (K_D) value of 6.99×10^2 M^{-1} were obtained.

- DNA nanostructure meets nanofabrication
  Zhang, G.; Surwade, S. P.; Zhou, F.; Liu, H. *Chem. Soc. Rev.* **2013**, *42*, 2488-2496.
  Abstract:

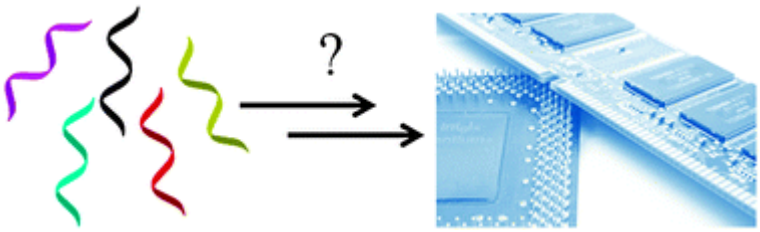

Recent advances in DNA nanotechnology have made it possible to construct DNA nanostructures of almost arbitrary shapes with 2–3 nm of precision in their dimensions. These DNA nanostructures are ideal templates for bottom-up nanofabrication. This review highlights the challenges and recent advances in three areas that are directly related to DNA-based nanofabrication: (1) fabrication of

large scale DNA nanostructures; (2) pattern transfer from DNA nanostructure to an inorganic substrate; and (3) directed assembly of DNA nanostructures.

- Are Quantum Dots Toxic? Exploring the Discrepancy Between Cell Culture and Animal Studies
  Tsoi, K. M.; Dai, Q.; Alman, B. A.; Chan, W. C. W. *Acc. Chem. Res.* **2013**, *46*, 662–671.
  Abstract:

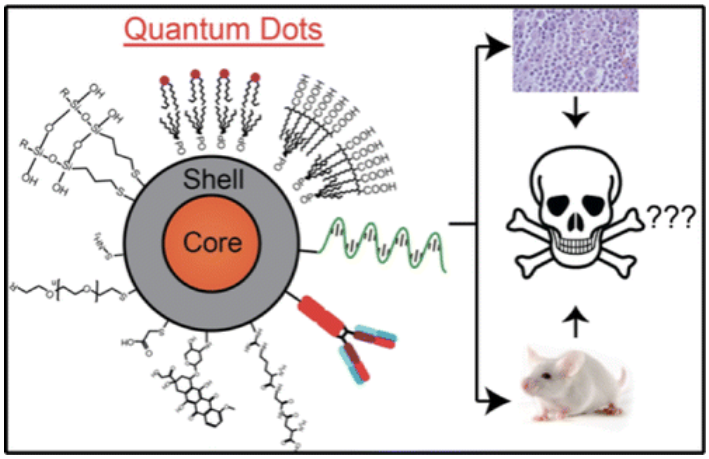

Despite significant interest in developing quantum dots (QDs) for biomedical applications, many researchers are convinced that QDs will never be used for treating patients because of their potential toxicity. The perception that QDs are toxic is rooted in two assumptions. Cadmium-containing QDs can kill cells in culture. Many researchers then assume that because QDs are toxic to cells, they must be toxic to humans. In addition, many researchers classify QDs as a homogeneous group of materials. Therefore, if CdSe QDs are harmful, they extrapolate this result to all QDs. Though unsubstantiated, these assumptions continue to drive QD research. When dosing is physiologically appropriate, QD toxicity has not been demonstrated in animal models. In addition, QDs are not uniform: each design is a unique combination of physicochemical properties that influence biological activity and toxicity. In this Account, we summarize key findings from in vitro and in vivo studies, explore the causes of the discrepancy in QD toxicological data, and provide our view of the future direction of the field.

In vitro and in vivo QD studies have advanced our knowledge of cellular transport kinetics, mechanisms of QD toxicity, and biodistribution following animal injection. Cell culture experiments have shown that QDs undergo design-dependent intracellular localization and they can cause cytotoxicity by releasing free cadmium into solution and by generating free radical species. In animal experiments, QDs preferentially enter the liver and spleen following intravascular injection, undergo minimal excretion if larger than 6 nm, and appear to be safe to the animal.

In vitro and in vivo studies show an apparent discrepancy with regard to toxicity. Dosing provides one explanation for these findings. Under culture conditions, a cell experiences a constant QD dose, but the in vivo QD concentration can vary, and the organ-specific dose may not be high enough to induce detectable toxicity. Because QDs are retained within animals, long-term toxicity may be a problem but has not been established.

Future QD toxicity studies should be standardized and systematized because methodological variability in the current body of literature makes it difficult to compare and contrast results. We advocate the following steps for consistent, comparable toxicology data: (a) standardize dose metrics, (b) characterize QD uptake concentration, (c) identify in vitro models that reflect the cells QDs interact with in vivo, and (d) use multiple assays to determine sublethal toxicity and biocompatibility.

Finally, we should ask more specific toxicological questions. For example: “At what dose are 5 nm CdSe QDs that are stabilized with mercaptoacetic acid and conjugated to the antibody herceptin toxic to HeLa cells?” rather than “Are QDs toxic?” QDs are still a long way from realizing their potential as a medical technology. Modifying the current QD toxicological research paradigm, investigating toxicity in a case-by-case manner, and improving study quality are important steps in identifying a QD formulation that is safe for human use.

- Bio-Based Furan Polymers with Self-Healing Ability
  Zeng, C.; Seino, H.; Ren, J.; Hatanaka, K.; Yoshie, N. *Macromolecules* **2013**, *46*, 1794-1802.
  Abstract:

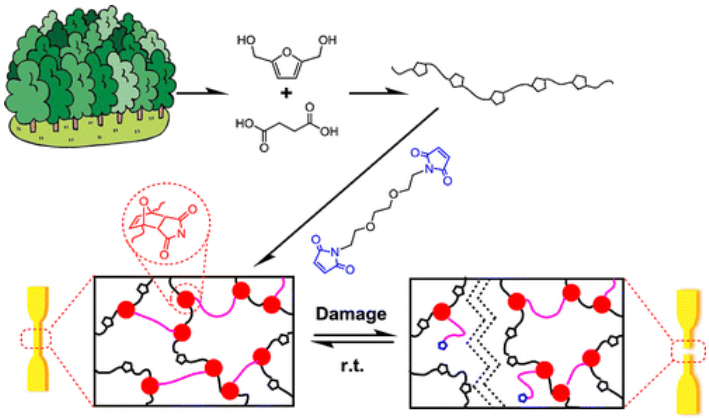

We report the preparation of a furan polymer, poly(2,5-furandimethylene succinate) by means of a condensation reaction between bio-based monomers. A reversible Diels-Alder reaction between furan and maleimide groups allowed the formation of network polymers cross-linked by a bismaleimide. By controlling the amount of the bismaleimide, mechanical properties were varied widely. These network polymers healed well when their broken surfaces were activated by bismaleimide solutions or solvent. The polymers also displayed excellent self-healing ability without external stimulus. This polymer class offers a wide range of possibilities to produce materials from biomass that have both practical mechanical properties and healing ability. These materials have the potential to bring great benefits to our daily lives by enhancing the safety, performance, and lifetime of products.

- Shape Memory Assisted Self-Healing Coating
  Luo, X.; Mather, P. T. *ACS Macro Lett.* **2013**, *2*, 152-156.
  Abstract:

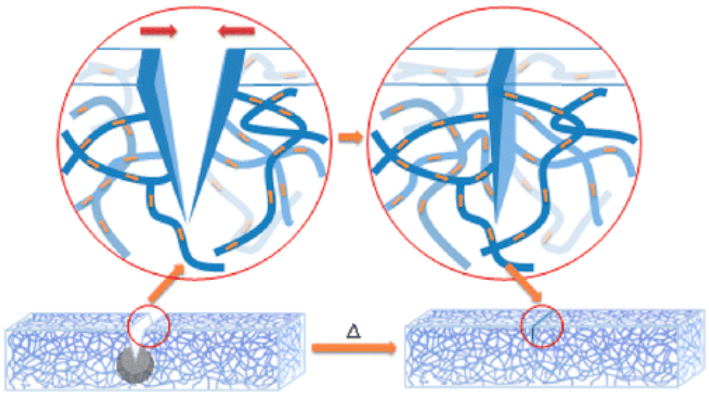

In this communication, we report the preparation and characterization of new shape memory

assisted self-healing (SMASH) coatings. The coatings feature a phase-separated morphology with electrospun thermoplastic poly(ε-caprolactone) (PCL) fibers randomly distributed in a shape memory epoxy matrix. Mechanical damage to the coating can be self-healed via heating, which simultaneously triggers two events: (1) the shape recovery of the matrix to bring the crack surfaces in spatial proximity, and (2) the melting and flow of the PCL fibers to rebond the crack. In controlled healing experiments, damaged coatings not only heal structurally, but also functionally by almost completely restoring the corrosion resistance. We envision the wide applicability of the SMASH concept in designing the next-generation self-healing materials.

- Effects of Impurities on Operational Mechanism of Organic Bulk Heterojunction Solar Cells
  Kaake, L.; Dang, X.-D.; Leong, W. L.; Zhang, Y.; Heeger, A.; Nguyen, T.-Q. *Adv. Mater.* **2013**, *25*, 1706–1712.
  Abstract:

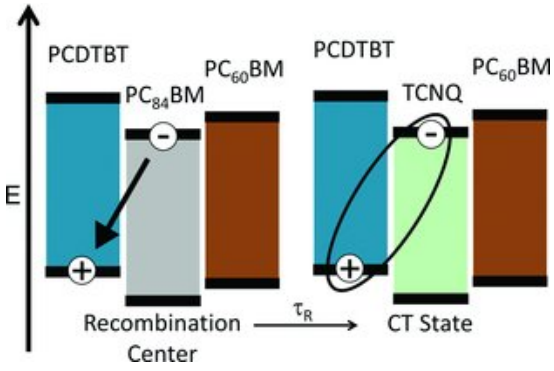

Photoconductive atomic force microscopy in conjunction with transient absorption spectroscopy and charge transport study were used to investigate the effect of impurities (TCNQ and $PC_{84}BM$) on the performance of low band gap conjugated polymer and fullerene solar cells to gain insight into whether differing impurity shapes may lead to different loss mechanisms.

- Self-Assembled, Nanowire Network Electrodes for Depleted Bulk Heterojunction Solar Cells
  Lan, X.; Bai, J.; Masala, S.; Thon, S. M.; Ren, Y.; Kramer, I. J.; Hoogland, S.; Simchi, A.; Koleilat, G. I.; Paz-Soldan, D.; Ning, Z.; Labelle, A. J.; Kim, J. Y.; Jabbour, G.; Sargent, E. H. *Adv. Mater.* **2013**, *25*, 1769–1773.
  Abstract:

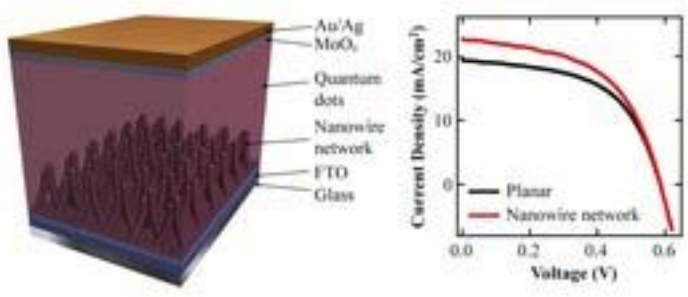

Herein, a solution-processed, bottom-up-fabricated, nanowire network electrode is developed. This electrode features a ZnO template which is converted into locally connected, infiltratable, TiO_2 nanowires. This new electrode is used to build a depleted bulk heterojunction solar cell employing hybrid-passivated colloidal quantum dots. The new electrode allows the application of a thicker, and thus more light-absorbing, colloidal quantum dot active layer, from which charge extraction of an efficiency comparable to that obtained from a thinner, planar device could be obtained.

- Highly Selective Dispersion of Carbon Nanotubes by Using Poly(phenyleneethynylene)-Guided Supermolecular Assembly
  Chen, Y.; Xu, Y.; Wang, Q.; Gunasinghe, R. N.; Wang, X-Q.; Pang, Y. *Small* **2013**, *9*, 870–875.
  Abstract:

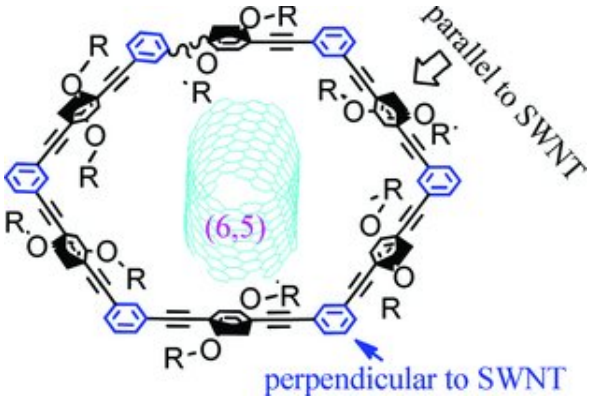

Isolation of single-walled carbon nanotubes (SWNTs) with specific chirality and diameters is critical for achieving optimum performance of SWNTs in various applications. A water-soluble π-conjugated polymer, poly[(m-phenyleneethynylene)-alt-(p-phenyleneethynylene)], 3, is found to exhibit high selectivity in dispersing SWNT (6,5). The polymer's ability to sort out SWNT (6,5) appears to be related to the carbon–carbon triple bond, whose free rotation allows a unique assembly of chromophores in a helical conformation. The observation is consistently supported by fluorescence, Raman, and UV-vis-NIR absorption spectra. The intriguing selectivity of 3 to SWNT (6,5), however, is not observed for the vinylene analogue polymer 1, showing that the carbon–carbon triple bond could play a unique role in sorting out a specific SWNT. The observed selectivity from 3 could be attributed to a combination of the helical cavity size restrain and electronic interaction associated with the local chromophore arrangement. This strategy could be expanded for efficient SWNT sorting when the helical conformation is further finely tuned.Rapid, Controllable Fabrication of Regular Complex Microarchitectures by Capillary Assembly of Micropillars and Their Application in Selectively Trapping/Releasing Microparticles

- Microstructured, Functional PVA Hydrogels through Bioconjugation with Oligopeptides under Physiological Conditions
  Chong, S-F.; Smith, A. A. A.; Zelikin, A. N. *Small* **2013**, *9*, 942–950.
  Abstract:

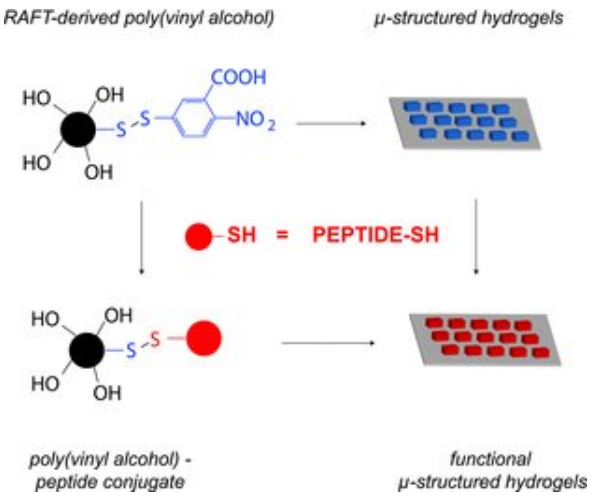

In this work, bioconjugation techniques are developed to achieve peptide functionalization of poly(vinyl alcohol), PVA, as both a polymer in solution and within microstructured physical hydrogels, in both cases under physiological conditions. PVA is unique in that it is one of very few polymers with excellent biocompatibility and safety and has FDA approval for clinical uses in humans. However, decades of development have documented only scant opportunities in bioconjugation with PVA. As such, materials derived thereof fail to answer the call for functional biomaterials for advanced cell culture and tissue engineering applications. To address these limitations, PVA is synthesized with terminal thiol groups and conjugated with thiolated peptides using PVA in solution. Further, microstructured, surface-adhered PVA physical hydrogels are assembled, the available conjugation sites within the hydrogels are quantified, and quantitative kinetic data are collected on peptide conjugation to the hydrogels. The success of bioconjugation in the gel phase is quantified through the use of a cell-adhesive peptide and visualization of cell adhesion on PVA hydrogels as cell culture substrates. Taken together, the presented data establish a novel paradigm in bioconjugation and functionalization of PVA physical hydrogels. Coupled with an excellent safety profile of PVA, these results deliver a superior biomaterial for diverse biomedical applications.

- Flexible Minerals: Self-Assembled Calcite Spicules with Extreme Bending Strength
  Natalio, F., Corrales, T. P.; Panthöfer, M.; Schollmeyer, D.; Lieberwirth, I.; Müller, W. E. G.; Kappl, M.; Butt, H.-J.; Tremel, W. *Science* **2013**, *339*, 1298-1302.
  Abstract:

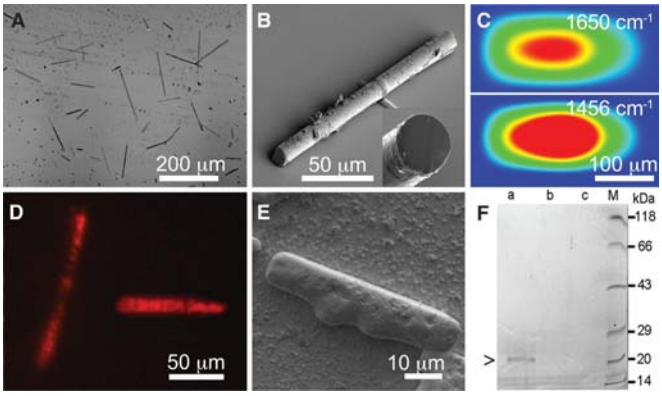

Silicatein-α is responsible for the biomineralization of silicates in sponges. We u sed silicatein-α to guide the self-assembly of calcite "spicules" similar to the spicules of the calcareous sponge *Sycon* sp. The self-assembled spicules, 10 to 300 micrometers (µm) in length and 5 to 10 µm in diameter, are composed of aligned calcite nanocrystals. The spicules are initially amorphous but transform into calcite within months, exhibiting unusual growth along [100]. They scatter x-rays like twinned calcite crystals. Whereas natural spicules evidence brittle failure, the synthetic spicules show an elastic response, which greatly enhances bending strength. This remarkable feature is linked to a high protein content. With nano-thermogravimetric analysis, we measured the organic content of a single spicule to be 10 to 16%. In addition, the spicules exhibit waveguiding properties even when they are bent.

- Real-Time Observation of Surface Bond Breaking with an X-ray Laser
  Dell'Angela, M.; Anniyev, T.; Beye, M.; Coffee, R.; Föhlisch, A.; Gladh, J.; Katayama, T.; Kaya, S.; Krupin, O.; LaRue, J.; Møgelhøj, A.; Nordlund, D.; Nørskov, J. K.; Öberg, H.; Ogasawara, H.; Öström, H.; Pettersson, L. G. M.; Schlotter, W. F.; Sellberg, J. A.; Sorgenfrei, F.; Turner, J. J.;

Wolf, M.; Wurth, W.; Nilsson, A. *Science* **2013**, *339*, 1302-1305.

Abstract:

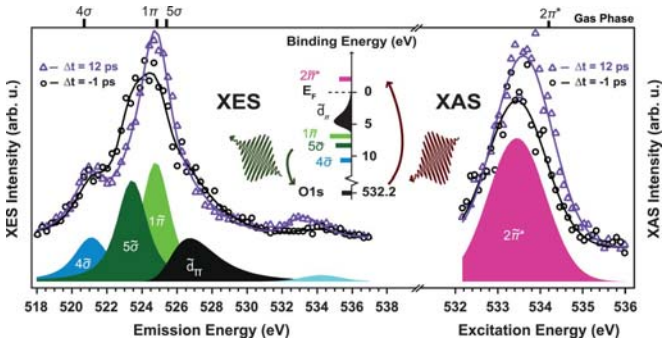

We used the Linac Coherent Light Source free-electron x-ray laser to probe the electronic structure of CO molecules as their chemisorption state on Ru(0001) changes upon exciting the substrate by using a femtosecond optical laser pulse. We observed electronic structure changes that are consistent with a weakening of the CO interaction with the substrate but without notable desorption. A large fraction of the molecules (30%) was trapped in a transient precursor state that would precede desorption. We calculated the free energy of the molecule as a function of the desorption reaction coordinate using density functional theory, including van der Waals interactions. Two distinct adsorption wells—chemisorbed and precursor state separated by an entropy barrier—explain the anomalously high prefactors often observed in desorption of molecules from metals.